Orbital Fluctuation Theory in Iron Pnictides: Effects of As-Fe-As Bond Angle, Isotope Substitution, and Z^2-Orbital Pocket on the Superconductivity

Tetsuro SAITO[1], Seiichiro ONARI[2], and Hiroshi KONTANI[1]
[1] *Department of Physics, Nagoya University and JST, TRIP, Furo-cho, Nagoya 464-8602, Japan.*
[2] *Department of Applied Physics, Nagoya University and JST, TRIP, Furo-cho, Nagoya 464-8602, Japan.*
(Dated: October 18, 2010)

We study the pairing mechanism in iron pnictide superconductors based on the five-orbital Hubbard-Holstein model. Due to Fe-ion oscillations, the s-wave superconducting (SC) state without sign reversal (s_{++}-wave state) is induced by orbital fluctuations by using realistic model parameters. The virtue of the present theory is that the famous empirical relation between T_c and the As-Fe-As bond angle is automatically explained, since the electron-phonon (e-ph) coupling that creates the orbital fluctuations is the strongest when the As_4-tetrahedron is regular. The negative iron isotope effect is also reproduced. In addition, the magnitude of the SC gap on hole-pockets is predicted to be rather insensitive to the corresponding d-orbital (xz/yz- or z^2-orbital), which is consistent with the recent bulk-sensitive angle-resolved photoemission spectroscopy (ARPES) measurement for $(Ba,K)Fe_2As_2$ and $BaFe_2(As,P)_2$. These obtained results indicate that the orbital-fluctuation-mediated s_{++}-wave state is a plausible candidate for iron pnictides.

PACS numbers: 74.70.Xa, 74.20.-z, 74.20.Rp

I. INTRODUCTION

The understanding of the pairing mechanism in iron pnictide superconductors [1] has been a significant open problem. By taking account of the Coulomb interaction at Fe-ions and the nesting of the Fermi surfaces (FSs), a fully-gapped sign-reversing s-wave state ($s_{\pm}$-wave state) has been proposed based on the spin fluctuation theories [2, 3]. Up to now, spin-fluctuation-mediated unconventional superconductivity is believed to be realized in various metals, such as high-T_c cuprates [4–6], κ-(BEDT-TTF)$_2$X [7–9], and CeMIn$_5$ (M=Co,Rh,Ir) [10]. To confirm the spin-fluctuation scenario in iron pnictides, it is of significant importance to find evidences for the sign-reversal in the superconducting (SC) gap, and for the relationship between spin fluctuation strength and the SC transition temperature T_c.

In principle, spin-fluctuation-mediated superconductivity is fragile against nonmagnetic impurities or randomness, since the SC gap function has sign changes inevitably. This is also true for iron pnictides, although the FSs are disconnected and the SC gap is fully-gapped. According to Ref. [11], decrease in T_c per $\rho_{\rm imp} = 1\mu\Omega$cm reaches $\sim$ 1K *independently of the impruity potential strength*. Contrary to this expectation, the SC state is very robust against various impurities [12] and heavy-particle irradiations [13, 14], although carrier number dependence may exist [15]. Moreover, the spin-fluctuation-mediated superconductors are expected to show a "resonance peak" in the neutron inelastic scattering as a reflection of sign-change in the SC gap, as observed in high-T_c cuprates [16–18] and in CeMIn$_5$ (M=Co,Rh,Ir) [19]. However, the observed "resonance-like" peak structure in iron pnictides [20–22] is reproduced theoretically by considering the strong correlation effect via quasiparticle damping, even in the conventional s-wave state without sign reversal (s_{++}-wave state) [23].

In $BaFe_2(As_{1-x}P_x)_2$, T_c increases as x decreases till the lattice structure transition occurs at $x = 0.27$, and T_c is positively correlated to the spin-fluctuation strength for $x \geq 0.33$ [24]. On the other hand, T_c in $LaFeAsO_{1-x}F_x$ at $x = 0.14$ increases from 26 K to 43 K by applying the pressure, whereas spin-fluctuation strength observed by $1/T_1T$ measurement is almost unchanged [25]. Thus, the correlation between the spin-fluctuation strength and T_c seems to depend on compounds.

Considering these difficulties in the $s_{\pm}$-wave scenario, we have proposed the orbital-fluctuation theory in Ref. [26], by taking account of the d-orbital degree of freedom in iron pnictides. It was found that large orbital fluctuations are induced by the electron-phonon (e-ph) interaction due to Fe-ion oscillations, although they are not induced by Coulomb interaction alone. Then, orbital-fluctuation-mediated s_{++}–wave SC state is realized [26, 27] even if e-ph interaction is smaller than that estimated by the first principle study [28]. Existence of large ferro-orbital fluctuations is suggested by prominent softening of shear modulus in Ba122 [29, 30]. Also, Raman spectroscopy [31], angle-resolved photoemission spectroscopy (ARPES) [32], and optical conductivity measurement [33] highlight the importance of e-ph interaction.

In this paper, we analyze the five-orbital Hubbard-Holstein (HH) model for iron pnictides in detail, by taking account of all the matrix elements of the e-ph interaction due to Fe-ion oscillations correctly. It is found that a small e-ph interaction ($\lambda \lesssim 0.15$) can induce substantial orbital fluctuations, utilizing all five d-orbitals on the FSs efficiently. Our main findings are as follows: (i) Empirical relation between T_c and the As-Fe-As bond angle (Lee plot) [34] is automatically explained, (ii) Experimental negative isotope effect [35] is reproduced, (iii) Magnitude of the SC gap on the Z^2-orbital hole-pocket

in (Ba,K)Fe_2As_2 and $BaFe_2(As,P)_2$ is comparable to the gap on other hole-pockets, which is consistent with experiments [36]. The range of model parameters for the s_{++}-wave SC state becomes wider in the presence of small amount of nonmagnetic impurities [11]. In addition, the predicted orbital fluctuations had been observed as the softening of the elastic constants C_{44} and C_E in Ref. [30].

Here, we consider the "orbital physics" in iron pnictides: It has been revealed that the ordered phase in mother compounds is not a simple spin-density-wave (SDW) state, but prominent orbital-density-wave coexists. In fact, recent bulk-sensitive ARPES in $BaFe_2As_2$ below T_N had shown that the Fermi surface around Γ-point are mainly composed of xz-orbital, indicating the prominent nonequivalence between xz- and yz-orbitals at the Fermi level in mother compounds [37]. Also, apparent in-plane anisotropy of resistivity had been observed in detwinned Ba122 even above the structural transition temperature (T_s), suggesting the existence of nematic order as a pure electronic origin [38]. These experimental facts indicate the existence of orbital fluctuations even in (doped) superconducting compounds, and therefore orbital-fluctuation-mediated s_{++}-wave SC state is expected to occur next to the orbital-density-wave state in iron pnictides.

II. MODEL AND HAMILTONIAN

We construct the five orbital HH model for iron pnictides, by adding the electron-phonon (e-ph) interaction to the Hubbard model in Ref.[2]. The Hubbard model is comprised of the potential term ϵ_μ, hopping term $t_{ij}^{\mu\nu}$, intraorbital Coulomb U, interorbital Coulomb U', Hund's coupling J, and pair hopping J'; [2]

$$\begin{aligned} H_{\rm Hub} &= \sum_i \sum_\mu \sum_\sigma \epsilon_\mu n_{i\mu\sigma} + \sum_{ij} \sum_{\mu\nu} \sum_\sigma t_{ij}^{\mu\nu} c_{i\mu\sigma}^\dagger c_{j\nu\sigma} \\ &+ \sum_i \Bigg(U \sum_\mu n_{i\mu\uparrow} n_{i\mu\downarrow} + U' \sum_{\mu>\nu} \sum_{\sigma\sigma'} n_{i\mu\sigma} n_{i\nu\sigma'} \\ &- J \sum_{\mu\neq\nu} \boldsymbol{S}_{i\mu} \cdot \boldsymbol{S}_{i\nu} + J' \sum_{\mu\neq\nu} c_{i\mu\uparrow}^\dagger c_{i\mu\downarrow}^\dagger c_{i\nu\downarrow} c_{i\nu\uparrow} \Bigg), \quad (1) \end{aligned}$$

where i,j denote the sites, and μ,ν are the five d-orbitals. We denote Z^2, XZ, YZ, X^2-Y^2, and XY orbitals as 1, 2, 3, 4, and 5 respectively: The X- and Y-axes are parallel to the nearest Fe-As bonds, and Z-axis is perpendicular to the FeAs plane [2]. The XY-coordinate is given by -45° rotation of the xy-coordinate spanned by the nearest Fe-Fe bonds around the z-axis.

Now, we derive the e-ph interaction term due to the Einstein oscillation of Fe ions. The Coulomb potential for the d electron at $\boldsymbol{r}$ (with the origin at the center of the Fe ion) due to the surrounding As^{3-}-ion tetrahedron is given by [26],

$$\begin{aligned} \phi^\pm(\boldsymbol{r};\boldsymbol{u}) &= 3e^2 \sum_{s=1}^4 \left\{ \left|\boldsymbol{r}+\boldsymbol{u}-\boldsymbol{R}_s^\pm\right|^{-1} - \left|\boldsymbol{r}-\boldsymbol{R}_s^\pm\right|^{-1} \right\} \\ &\approx \pm A \left[2XZ \cdot u_X - 2YZ \cdot u_Y + (X^2-Y^2) u_Z \right], \quad (2) \end{aligned}$$

where $\boldsymbol{u}$ is the displacement vector of the Fe ion, $\boldsymbol{R}_s^\pm$ is the location of surrounding As ions in Fig. 1 (a); When As_4 tetrahedron is regular tetrahedron ($\alpha = 109.47^\circ$), $a=\sqrt{2/3}$ and $b=\sqrt{1/3}$. That is, $\boldsymbol{R}^+/R_{\text{Fe-As}} = (\pm a, 0, b)$ and $(0, \pm a, -b)$ for $Fe^{(1)}$, and $\boldsymbol{R}^-/R_{\text{Fe-As}} = (\pm a, 0, -b)$ and $(0, \pm a, b)$ for $Fe^{(2)}$, and $A = 30e^2/\sqrt{3}R_{\text{Fe-As}}^4$. $R_{\text{Fe-As}}$ is the Fe-As bond length. We neglect the As-ion oscillations since they do not induce substantial orbital fluctuations unless very large e-ph interaction is assumed.

Nonzero matrix elements $\langle\mu|\phi|\nu\rangle = \sum_\Xi^{XYZ} v_{\mu\nu}^\Xi u_\Xi$ are given as

$$\begin{aligned} v_{24}^X = v_{35}^X &= \pm 2Aa^2/7, \\ v_{34}^Y = -v_{25}^Y &= \pm 2Aa^2/7, \\ v_{22}^Z = -v_{33}^Z &= \pm 2Aa^2/7, \\ v_{12}^X &= \pm 2Aa^2/7 \cdot (1/\sqrt{3}), \\ v_{13}^Y &= \mp 2Aa^2/7 \cdot (1/\sqrt{3}), \\ v_{14}^Z &= \mp 2Aa^2/7 \cdot (2/\sqrt{3}), \end{aligned} \quad (3)$$

where a is the radius of d orbital. The obtained e-ph interaction does not couple to the charge density since $v_{\mu\nu}^\Xi$ is trace-less. Thus, the Thomas-Fermi screening for the coefficient A is absent. We stress that there are many nonzero (off-diagonal) elements in Eq. (3) due to the fact that As ions locate out of the Fe plane. Then, the e-ph interaction term is given by

$$H_{e-\text{ph}} = \sum_i \sum_{\mu\nu} \sum_\Xi \sum_\sigma v_{\mu\nu}^\Xi c_{i\mu\sigma}^\dagger c_{i\nu\sigma} u_{i\Xi}, \quad (4)$$

which represents the orbital exchange process induced by the Fe ion displacement. We will show later that substantial orbital fluctuations involving all five orbitals are developed because of many nonzero elements in Eq. (3).

Next, we derive the phonon-mediated electron-electron interaction. The local phonon Green function is

$$D(\omega_l) = \frac{2\bar{u}_0^2 \omega_D}{\omega_l^2 + \omega_D^2}, \quad (5)$$

which is the Fourier transformation of $\langle T_\tau u_\mu(\tau) u_\mu(0)\rangle$ ($\mu = X, Y, Z$). ω_D is the phonon frequency, and $\bar{u}_0 = \sqrt{\hbar/2M_{\text{Fe}}\omega_D}$ is the uncertainty in position for Fe ions; $\bar{u}_0 = 0.044$ Å for $\omega_{\text{D}} = 0.02$ eV. $\omega_l = 2\pi l T$ is the boson Matsubara frequency.

For both $Fe^{(1)}$ and $Fe^{(2)}$, the phonon mediated interaction is obtained as

$$H_{\text{e-e}}^{\text{ph}} = \sum_{\mu\nu\mu'\nu'} \sum_i \sum_{\sigma\sigma'} V_{\mu\nu,\mu'\nu'}(\omega_l) c_{i\mu\sigma}^\dagger c_{i\nu\sigma} c_{i\mu'\sigma'}^\dagger c_{i\nu'\sigma'}. \quad (6)$$

In Eq. (6), nonzero $V_{\mu\nu,\mu'\nu'}$ are given as

$$\begin{aligned} V_{24,24} = V_{34,34} = V_{22,22} = V_{33,33} = -V_{22,33} = -g(\omega_l), \\ V_{25,25} = V_{35,35} = V_{24,35} = -V_{25,34} = -g(\omega_l), \\ V_{12,35} = V_{13,25} = V_{12,24} = -V_{13,34} = -(1/\sqrt{3})g(\omega_l), \\ V_{12,12} = V_{13,13} = -(1/3)g(\omega_l), \\ V_{14,33} = -V_{14,22} = -(2/\sqrt{3})g(\omega_l), \\ V_{14,14} = -(4/3)g(\omega_l), \end{aligned} \quad (7)$$

where $g(\omega_l) \equiv (2Aa^2/7)^2 D(\omega_l)$. The following relations hold; $V_{lm,l'm'} = V_{ml,l'm'} = V_{lm,m'l'}$ and $V_{lm,l'm'} = V_{l'm',lm}$. In our earlier investigation [26], we have estimated $g(0) \approx 0.4$eV for $R_{\mathrm{Fe-As}} \approx 2.4$ Å, $a \approx 0.77$ Å, and $\omega_D \approx 0.018$eV. We also obtain $g(0) \approx 0.33$eV for $\omega_D \approx 0.02$eV.

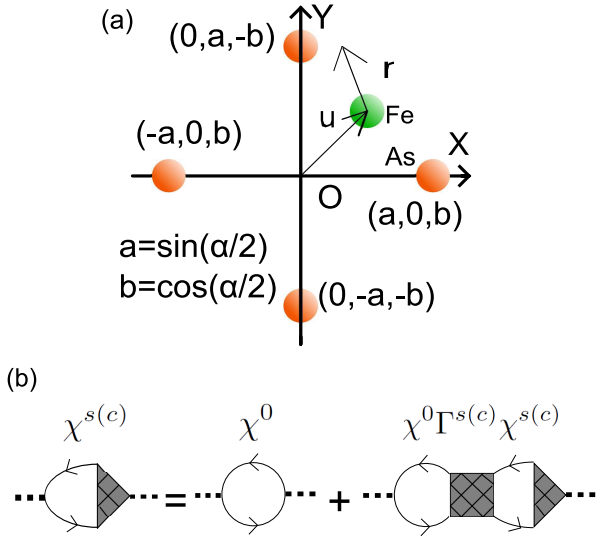

FIG. 1: (Color online) (a) As_4 tetrahedron in iron pnictides shown along the z axis. Here, we put $R_{\mathrm{Fe\text{-}As}} = 1$. The As-Fe-As bond angle α is illustrated in Fig. 6 (a). (b) The diagrammatic expression for $\chi^{s(c)}$.

In our earlier calculation [26], only the first line of Eq. (7) was taken into account since the weight of orbitals 1 and 5 on the FSs is small. In this paper, however, we will show later that orbital fluctuations increase substantially if all the interactions in Eq. (7) are taken into account correctly. This is one of the main message in the present work.

Now, we perform the RPA for $H_{\mathrm{Hub}} + H^{\mathrm{ph}}_{\mathrm{e\text{-}e}}$. The irreducible susceptibility in the five orbital model is given by

$$\chi^0_{ll',mm'}(q) = -\frac{T}{N}\sum_k G^0_{lm}(k+q)\, G^0_{m'l'}(k), \quad (8)$$

where $\hat{G}^0(k) = [i\epsilon_n + \mu - \hat{H}^0_{\boldsymbol{k}}]^{-1}$ is the d electron Green function in the orbital basis, $q = (\boldsymbol{q}, \omega_l)$, $k = (\boldsymbol{k}, \epsilon_n)$, and $\epsilon_n = (2n+1)\pi T$ is the fermion Matsubara frequency. μ is the chemical potential, and $\hat{H}^0_{\boldsymbol{k}}$ is the kinetic term of Eq. (1). Then, the susceptibilities for spin and charge sectors in the RPA are given by [39]

$$\hat{\chi}^s(q) = \frac{\hat{\chi}^0(q)}{1 - \hat{\Gamma}^s\hat{\chi}^0(q)}, \quad (9)$$

$$\hat{\chi}^c(q) = \frac{\hat{\chi}^0(q)}{1 - \hat{\Gamma}^c(\omega_l)\hat{\chi}^0(q)}, \quad (10)$$

where

$$\Gamma^s_{l_1l_2,l_3l_4} = \begin{cases} U, & l_1 = l_2 = l_3 = l_4 \\ U', & l_1 = l_3 \neq l_2 = l_4 \\ J, & l_1 = l_2 \neq l_3 = l_4 \\ J', & l_1 = l_4 \neq l_2 = l_3 \end{cases} \quad (11)$$

$$\hat{\Gamma}^c(\omega_l) = -\hat{C} - 2\hat{V}(\omega_l), \quad (12)$$

$$C_{l_1l_2,l_3l_4} = \begin{cases} U, & l_1 = l_2 = l_3 = l_4 \\ -U' + 2J, & l_1 = l_3 \neq l_2 = l_4 \\ 2U' - J, & l_1 = l_2 \neq l_3 = l_4 \\ J', & l_1 = l_4 \neq l_2 = l_3 \end{cases} \quad (13)$$

Here, we neglect the ladder-diagram for phonon-mediated interaction because of the relation $\omega_D \ll W_{\mathrm{band}}$[26, 27]. The Bethe-Salpeter equation for $\chi^{s(c)}$ is given in Fig. 1 (b).

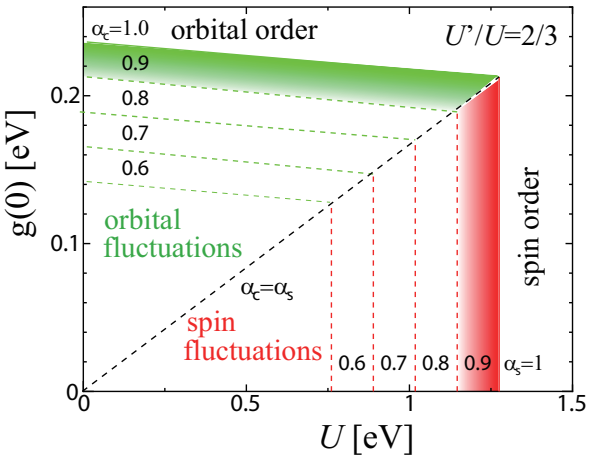

FIG. 2: (Color online) Obtained U-$g(0)$ phase diagram for $n = 6.1$. Near the orbital-density-wave boundary, s_{++}-wave SC state is realized by orbital fluctuations.

Hereafter, we assume that $J = J'$ and $U = U' + 2J$, and fix the ratio $J/U = 1/6$. Figure 2 shows the U-$g(0)$ phase diagram for $n = 6.1$ given by the RPA. $\alpha_{s(c)}$ is the spin (charge) Stoner factor, which is given by the maximum eigenvalue of $\hat{\Gamma}^{s(c)}\hat{\chi}^0(\boldsymbol{q}, 0)$. The transition line for the spin (orbital) order is given by the condition $\alpha_{s(c)} = 1$. Note that this phase diagram is independent of ω_D since

$\alpha_{s(c)}$ is free from ω_D. For $U = 1$ eV, the critical value $g_{\rm cr}(0)$ for $\alpha_c = 1$ is 0.22, which means that dimensionless coupling constant is $\lambda_{\rm cr} \equiv g_{\rm cr}(0)N(0) \sim 0.15$, where $N(0)$ is the density of states per spin at the Fermi level. Hereafter, the unit of energy is eV.

In our earlier work [26], we have shown that $g_{\rm cr}(0) \sim 0.4$ when only the first line of Eq. (7) is considered. However, we stress that $g_{\rm cr}(0)$ in Fig. 2 in the present paper is almost halved. This result means that strong orbital fluctuations are induced by much smaller $g(0)$ by utilizing all five d-orbitals on the FSs efficiently. Therefore, we take all the interaction in Eq. (7) into account in later calculations.

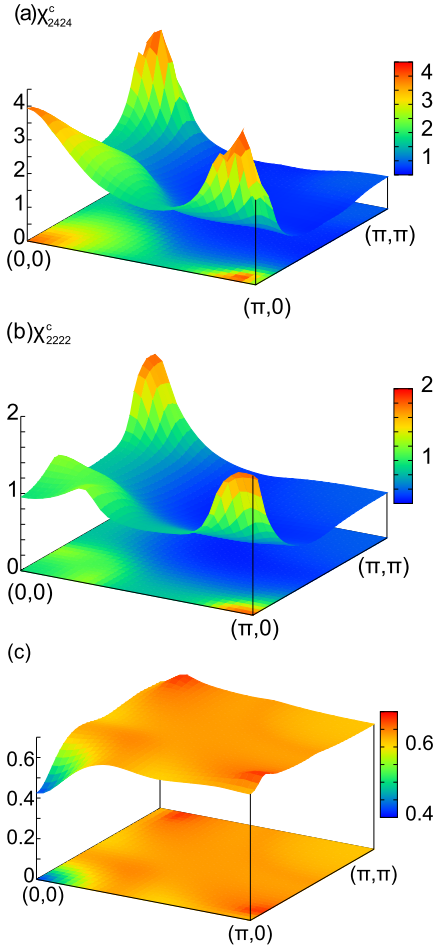

FIG. 3: (Color online) Obtained (a) $\chi^c_{24,24}(\boldsymbol{q},0)$ and (b) $\chi^c_{22,22}(\boldsymbol{q},0)$, for $n = 6.1$, $U = 1$, $T = 0.02$, and $g(0) = 0.21$. Note that $\chi^c_{24,24}(\boldsymbol{q},0) = \chi^c_{34,34}(\boldsymbol{q}',0)$ and $\chi^c_{22,22}(\boldsymbol{q},0) = \chi^c_{33,33}(\boldsymbol{q}',0)$, where $\boldsymbol{q}'$ is given by the rotation of $\boldsymbol{q}$ by $\pi/2$. In (c), charge susceptibility $\chi^c(\boldsymbol{q},0) \equiv \sum_{l,m}\chi^c_{ll,mm}(\boldsymbol{q},0)$ is shown. We use 2048 Matsubara frequencies.

Figure 3 shows the obtained $\chi^c_{ll',mm'}(\boldsymbol{q},0)$ for $(ll',mm') = (24,24)$ and $(22,22)$, respectively. Used parameters are $n = 6.1$, $U = 1$, $T = 0.02$, and $g(0) = 0.21$, which correspond to $\alpha_c = 0.98$. $\chi^c_{24,24}$ ($\chi^c_{34,34}$) and $\chi^c_{22,22}$ ($\chi^c_{33,33}$) are the most divergent channels for electron doped case. First, we discuss $\chi^c_{24,24}$ in Fig. 3 (a): It has the largest peak near $\boldsymbol{Q} = (\pi,0)$, which comes from the nesting between FS3,4 and FS1,2 in Fig. 4 (c), and the multiple scattering by $V_{24,24}$. Its second largest peak near $\boldsymbol{q} = (0,0)$ originates from the forward scattering by $V_{24,24}$ in the FS3 or FS4 that is composed of 2-4 orbitals. $\chi^c_{24,24}(\boldsymbol{0},0)$ and $\chi^c_{24,24}(\boldsymbol{Q},0)$ are comparable, meaning that the ferro-orbital and antiferro-orbital orders are highly frustrated. Note that $\chi^c_{24,24}(\boldsymbol{Q},0) \ll \chi^c_{24,24}(\boldsymbol{0},0)$ if we consider only the first line of Eq. (7) as demonstrated in Ref.[26].

We also discuss $\chi^c_{22,22}$ in Fig. 3 (b): It has the largest peak near $\boldsymbol{Q} = (\pi,0)$, which arises due to nesting between FS3,4 and FS1,2. $\chi^c_{22,22}$ also has a slightly lower peak around $(0,0)$ that originates from the forward scattering in each FS. We note that the large enhancement in $\chi^c_{24,24}$ and $\chi^c_{34,34}$ ($\chi^c_{22,22}$ and $\chi^c_{33,33}$) is caused by in-plane (out-of-plane) Fe-ion oscillations. On the other hand, the total charge susceptibility $\chi^c(\boldsymbol{q},0) \equiv \sum_{l,m}\chi^c_{ll,mm}(\boldsymbol{q},0)$ is not enhanced as shown in Fig. 3 (c), because of the relation $\chi^c_{22,22}(\boldsymbol{q},0) \approx -\chi^c_{22,33}(\boldsymbol{q},0)$ [26]. Therefore, the origin of the superconductivity in the present model is not charge fluctuations, but orbital fluctuations that can develop without cost of the Coulomb potential energy.

Finally, we discuss the softening in the elastic constants due to orbital fluctuations. Recently, Yoshizawa *et al.* have observed large softening in C_{44}, C_{66}, and $C_{\rm E}$ in $Ba(Fe,Co)_2As_2$ [30]. The corresponding strains for C_{44}, C_{66}, and $C_{\rm E}$ are ϵ_{XZ}, ϵ_{XY}, and $\epsilon_{XX} - \epsilon_{YY}$, respectively. Using the point-charge model, one can verify that the strains $\epsilon_{\mu\nu}$ $(\mu,\nu = X,Y,Z)$ induce the quadrupole potential on each Fe ion; $\phi_{\mu\nu} \propto \mu\nu$. The corresponding matrix elements $\langle l|\phi_{XZ}|m\rangle \equiv \phi^{XZ}_{lm}$ and $\langle l|\phi_{XX} - \phi_{YY}|m\rangle \equiv \phi^{X^2-Y^2}_{lm}$ are proportional to $|v^X_{lm}|$ and $|v^Z_{lm}|$, respectively, where v^Ξ_{lm} are described in Eq. (3). In the linear response theory, the enhancement in C^{-1}_{44} ($C^{-1}_{\rm E}$) is proportional to the quadrupole susceptibility $\sum_{ll'mm'}\phi^\Xi_{ll'}\chi^c_{ll',mm'}(\boldsymbol{0},0)\phi^\Xi_{mm'}$ with $\Xi = XZ$ ($\Xi = X^2 - Y^2$). As shown in Fig. 3, both $\chi^c_{24,24}$ and $\chi^c_{22,22}$ evolve in the present study. Considering that $\phi^{XZ}_{lm} \propto |v^X_{lm}|$ is finite for $l,m = 2,4$, we find that the softening in C_{44} is induced by fluctuations in the $(2,4)$-channel. In the same way, the softening in $C_{\rm E}$ is induced by fluctuations in $(2,2)$-, $(3,3)$-, and $(2,3)$-channels. These results are consistent with the reports in Ref. [30]. That is, theoretically predicted orbital fluctuations in Figs. 3 (a) and (b) had been confirmed experimentally.

III. ELIASHBERG GAP EQUATION

In this section, we analyze the following linearized Eliashberg equation using the RPA by taking account of both the spin and orbital fluctuations on the equal

footing [39]:

$$\lambda_E \Delta_{ll'}(k) = \frac{T}{N} \sum_{k',m_i} W_{lm_1,m_4l'}(k-k') G^0_{m_1m_2}(k') \times \Delta_{m_2m_3}(k') G^0_{m_4m_3}(-k'), \quad (14)$$

where,

$$\hat{W}(q) = -\frac{3}{2}\hat{\Gamma}^s\hat{\chi}^s\hat{\Gamma}^s + \frac{1}{2}\hat{\Gamma}^c\hat{\chi}^c\hat{\Gamma}^c - \frac{1}{2}(\hat{\Gamma}^s - \hat{\Gamma}^c), \quad (15)$$

for the singlet states. λ_E is the eigenvalue of the gap equation, which approaches unity as $T \to T_c$. Hereafter, we use 64^2 $\boldsymbol{k}$ meshes, and 1024 or 2048 Matsubara frequencies. We perform the calculation at relativity high temperatures ($T \geq 0.02$) since the number of meshes is not enough for $T < 0.02$.

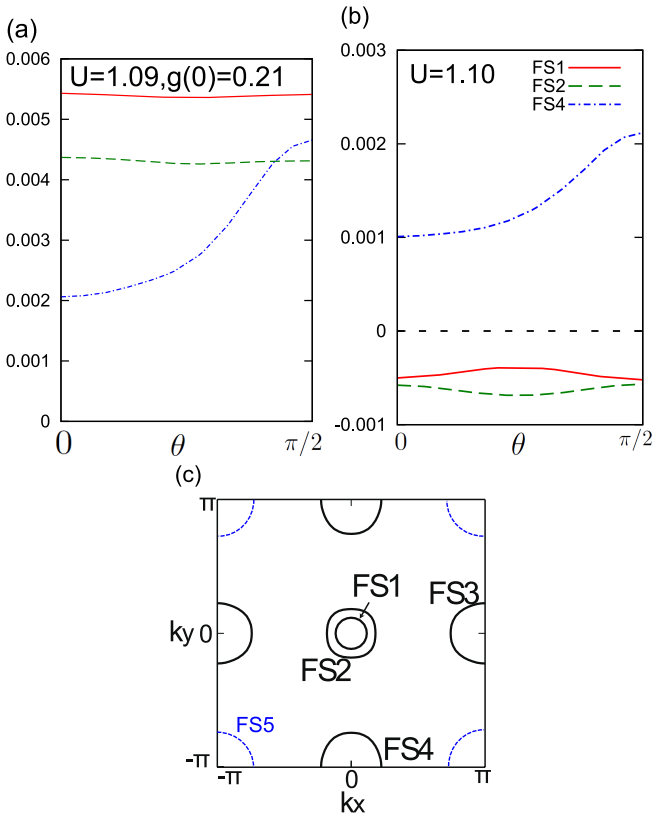

FIG. 4: (Color online) (a) (b) Obtained SC gap functions for (a)$U = 1.09$ and (b)$U = 1.10$, respectively. We put $g(0) = 0.21$ ($\alpha_c = 0.98$), $T = 0.02$, and $\omega_D = 0.02$. They are normalized as $N^{-1}\sum_{\boldsymbol{k},lm} |\Delta_{lm}(\boldsymbol{k})|^2 = 1$. We use 2048 Matsubara frequencies. (c) FSs in the unfolded Brillouin zone. FS1,2 (FS3,4) are composed of $2, 3$-orbitals ($2, 3, 4$-orbitals). FS5 is composed of 1-orbital in (Ba,K)Fe_2As_2 and $BaFe_2(As,P)_2$, which will be discussed in Sec. V A. Note that FS5 moves to $(0, 0)$ in the folded zone.

Figure 4 (a) and (b) show the SC gap on the FSs in the band representation for $U = 1.09$ and $U = 1.10$, respectively. We put $n = 6.1$, $T = 0.02$, $\omega_D = 0.02$, and $g(0) = 0.21$, which correspond to $\alpha_c = 0.98$. The horizontal axis is the azimuth angle for $\boldsymbol{k}$ point with the origin at Γ(M) point for FS1,2 (FS4). For $U = 1.09$, the s_{++} state is realized by orbital fluctuations [26]. On the other hand, the $s_{\pm}$ state is realized for $U = 1.10$ since the spin fluctuations dominate the orbital fluctuations. In this case, the boundary of the $s_{++} \to s_{\pm}$ phase transition is uniquely defined since the obtained gap functions are always full-gap. If one introduces low concentration of impurities, the s_{++}-wave state is realized even for $U > 1.1$ [26], and moreover, the transition becomes full-gap s_{++} →nodal s → full-gap $s_{\pm}$ [40]. For a quantitative study of the line nodes observed in several 122 compounds [41], the 3-dimensionality of the FSs may be indispensable.

Figure 5 shows the obtained λ_E for (a) $U = 0$ and (b) $U = 1$, respectively, at $T = 0.02$. In case (a), λ_E exceeds unity for $\omega_D = 0.02$ when $1 - \alpha_c \simeq 0.02$. λ_E increases as ω_D increases. Considering the relation $\omega_D \propto 1/\sqrt{M}$, this result means the positive isotope effect. In case (b), λ_E is larger than unity for $\omega_D = 0.02$ if $1 - \alpha_c \simeq 0.01$. We stress that λ_E decreases as ω_D increases, which means that the negative isotope effect is realized.

Now, we discuss the origin of the negative isotope effect in case (b). In the BCS theory, T_c in a single band model is given by [42]

$$T_c = 1.13\omega_D \exp\left(-\frac{1}{\lambda - \mu^*}\right), \quad (16)$$

where $\lambda = gN(0)$ is the dimensionless coupling constant, and μ^* is given as

$$\mu^* = \frac{\mu}{1 + \mu \ln(\bar{\epsilon}/\omega_D)}, \quad (17)$$

where $\mu = UN(0)$. μ^* is called the Morel-Anderson pseudo-potential. In general, $\mu^* \ll \mu$ since the limit of Coulomb interaction $\bar{\epsilon}$ is much larger than ω_D. Now, we derive the coefficient $\beta = -\partial \ln T_c / \partial \ln M$ ($T_c \propto M^{-\beta}$), where M is mass of Fe ion. By differentiating Eq. (16) by M using the relation $\omega_D \propto 1/\sqrt{M}$, we obtain

$$\beta = \frac{1}{2}\left[1 - \frac{\mu^{*2}}{(\lambda - \mu^*)^2}\right]. \quad (18)$$

The value of β decreases from $1/2$ as μ^* increases, and becomes negative when μ^* is larger than $\lambda/2$. This can be realized when U is relatively large. Therefore, the negative isotope effect ($\beta < 0$) in Fig. 5 (b) is caused by the reduction in μ^*. In other words, negative isotope effect originates from the enhancement of the retardation effect.

Note that Eq. (18) is valid only for one-band model. In order to obtain the correct coefficient β in iron pnictides, we have to analyze the five-orbital model.

In case of Fig. 5 (b), λ_E exceeds unity only when $\alpha_c \sim 0.99$. However, λ_E can reach unity for smaller α_c when the temperature is much lower than $\omega_D = 0.02$.

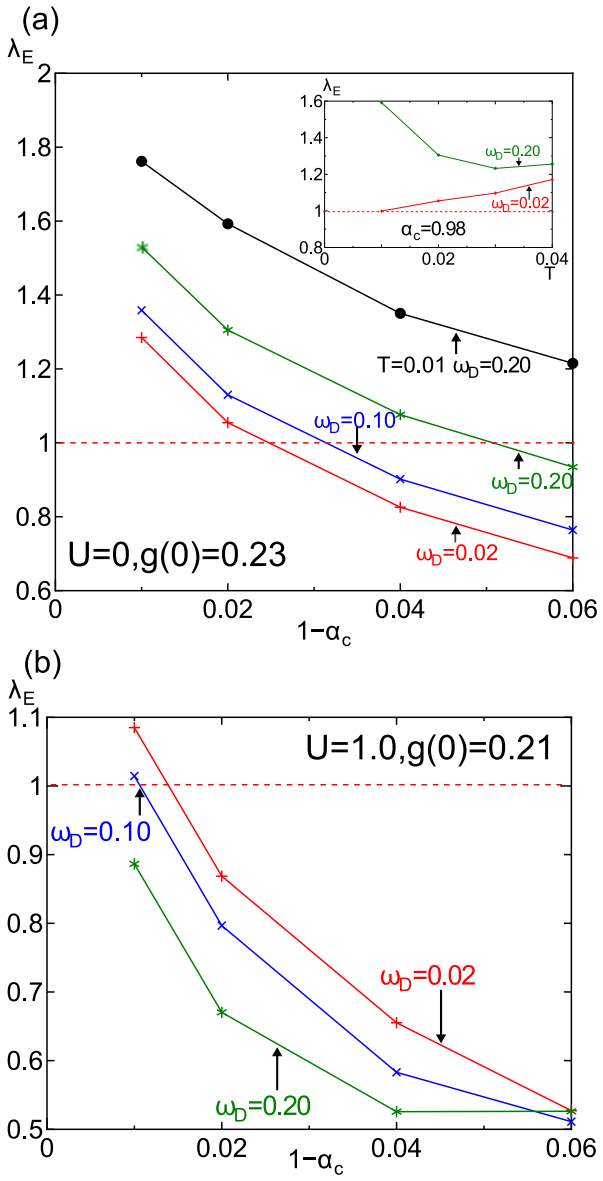

FIG. 5: (Color online) Obtained λ_E as function of $1-\alpha_c$ for (a)$U=0$ and (b)$U=1$, respectively, at $T=0.02$. The former (latter) corresponds to the positive (negative) isotope effect. We use 2048 Matsubara frequencies. Inset in (a): T-dependence of λ_E for $\alpha_c=0.98$.

To explain this behavior, we analyze the following single band gap equation [43]:

$$\lambda_E \Delta = T\sum_{\boldsymbol{k},n} \frac{\Delta}{\epsilon_n^2+\epsilon_{\boldsymbol{k}}^2} V(i\epsilon_n). \tag{19}$$

Here we consider the BCS approximation $V(k,i\epsilon_n) = -g\theta(\omega_D - |\epsilon_n - \pi T|)$. After carrying out the $\boldsymbol{k}$ summation, we obtain

$$\lambda_E \Delta = 2gN(0)\sum_{l=0}^{n_c} \frac{1}{2l+1}\Delta, \tag{20}$$

where $(2n_c+1)\pi T = \omega_D$. When $\omega_D \gg T$ (i.e. $n_c \gg 1$), Eq. (20) is solved as [43]:

$$\lambda_E = gN(0)\ln(1.13\omega_D/T). \tag{21}$$

Therefore, λ_E diverges logarithmically at low temperatures. On the other hand, when $\omega_D \simeq T$, Eq. (20) is solved by putting $n_c = 0$ as

$$\lambda_E = 2gN(0). \tag{22}$$

In this case, λ_E does not depend on T. Inset of Fig. 5 (a) shows the T-dependence of λ_E for $U=0$ and $g(0)=0.23$ ($\alpha_c = 0.98$). For $\omega_D = 0.20$, λ_E increases at low temperatures, in accordance with Eq. (21). In contrast, λ_E slightly decreases for $\omega_D = 0.02$ at low temperature, which might be due to the smaller size of $\boldsymbol{k}$- or ω-meshes. Unfortunately, we can not perform the calculation below 100K since the numbers of $\boldsymbol{k}$- and ω-meshes are not sufficient. However, even if $\omega_D = 0.02$, λ_E will increase below $T \sim 20$K. Therefore, λ_E is expected to exceed unity at low temperatures even if $\alpha_c \ll 0.99$.

Finally, we briefly discuss the effect of self-energy Σ, which has been dropped in the present study. The quasiparticle damping γ (= imaginary part of Σ) reduces both $\alpha_{s(c)}$ and $\lambda_{\rm E}$. However, the dimensionless coupling constant for $\alpha_c = 0.98$ in the FLEX approximation is only $\lambda \equiv g(0)N(0) \sim 0.2$ [40]. Thus, the present orbital-fluctuation scenario is justified even if the self-energy correction is taken into account. In the FLEX approximation, $g_{\rm cr}(0)$ for orbital-density-wave state and $U_{\rm cr}$ for SDW state become infinity in 2-dimensional systems since Mermin-Wagner theorem is satisfied [44].

IV. CRYSTAL STRUCTURE AND T_c

In previous sections, we assumed that the As_4 tetrahedron forms a regular tetrahedron. However, it is well-known that As-Fe-As bond angle α, which is shown in Fig. 6(a), closely relates on T_c experimentally [34]. Here, we extend the theory for general bond angle α. First, we derive the e-ph interaction for general α. In this case, the potential $\phi(\boldsymbol{r};\boldsymbol{u})$ in Eq. (2) is not changed except for A; A is changed as

$$A = \frac{30e^2}{\sqrt{3}R_{\text{Fe-As}}^4}\left(\frac{3\sqrt{3}}{2}\sin^2\frac{\alpha}{2}\cos\frac{\alpha}{2}\right). \tag{23}$$

When the As_4 tetrahedron forms the regular tetrahedron ($\alpha = \alpha_0 \equiv 109.47°$), the term in the brackets in Eq. (23) takes the maximum value; unity. Thus, the effective interaction for α is given by $g(0,\alpha) = g(0)[(3\sqrt{3}/2)\sin^2(\alpha/2)\cos(\alpha/2)]^2$, where $g(0) \equiv g(0,\alpha_0)$ In Fig. 6(b), we show $g(0,\alpha)/g(0)$ as a function of α. When α deviates from α_0, A^2 decreases rapidly.

Figure 7 shows the obtained $\chi^c_{22,22}(\boldsymbol{q},0)$ and $\chi^c_{24,24}(\boldsymbol{q},0)$ for $\alpha = 120°$, which corresponds to LaFePO. We put $g(0) = 0.21$, $U=1$, and $T=0.02$, which are

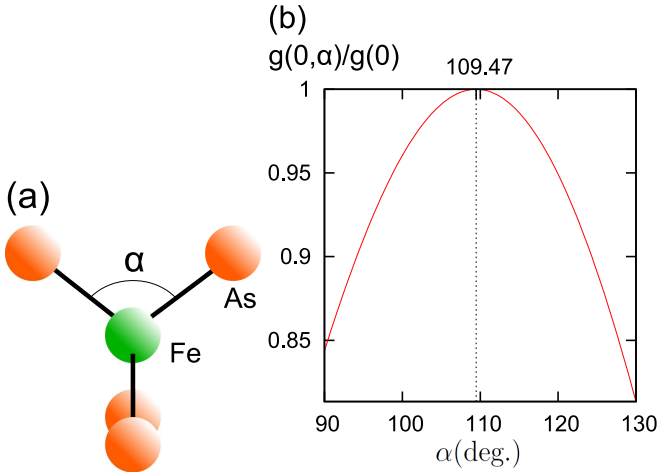

FIG. 6: (Color online) (a) The definitions of the As-Fe-As bond angle α. (b) $g(0,\alpha)/g(0)$ as a function of α.

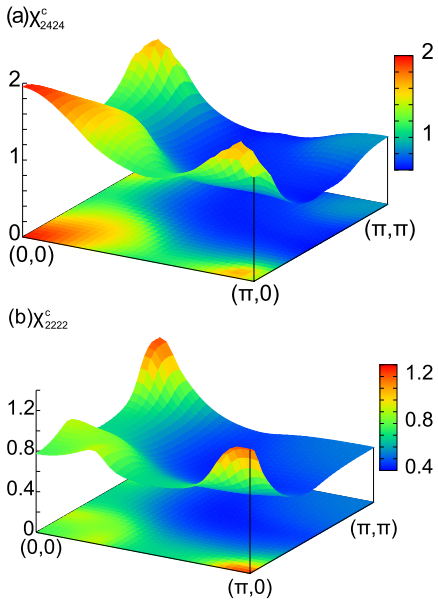

FIG. 7: (Color online) Obtained (a) $\chi^c_{24,24}(\boldsymbol{q},0)$ and (b) $\chi^c_{22,22}(\boldsymbol{q},0)$ for $\alpha = 120°$, $g(0) = 0.21$, $U = 1$, and $T = 0.02$. We use 1024 Matsubara frequencies.

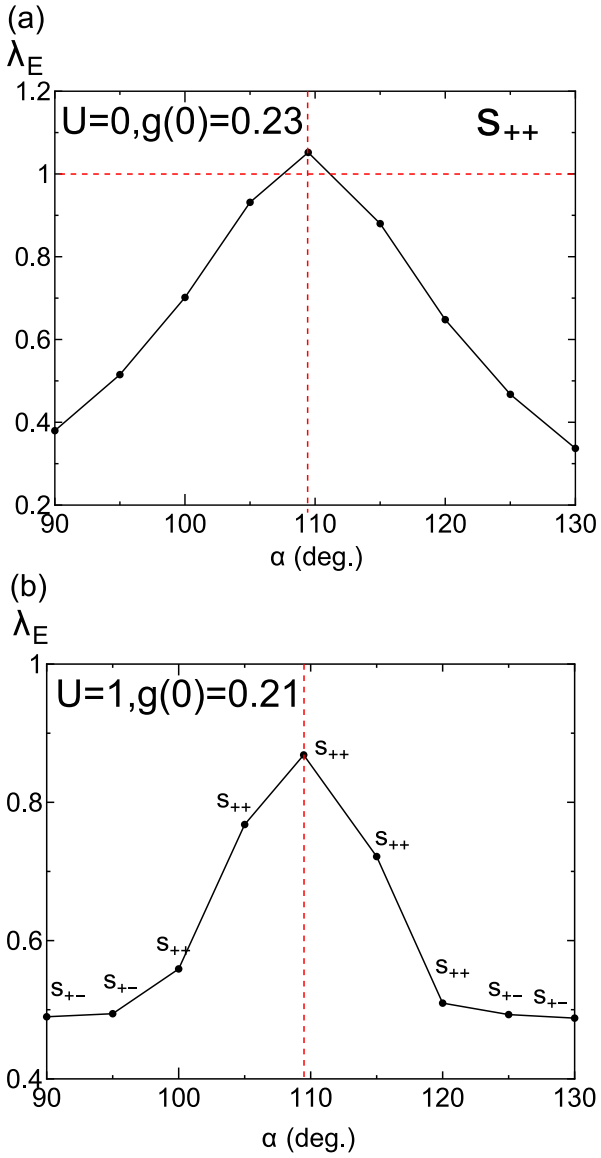

FIG. 8: (Color online) α-dependence of λ_E for (a)$U = 0$ and $g(0) = 0.23$, and (b)$U = 1$ and $g(0) = 0.21$, respectively. We put $T = 0.02$, and $\omega_D = 0.02$. In (a), s_{++}-wave state is always realized. We use 1024 Matsubara frequencies.

equivalent to those in Fig. 3. Here $\alpha_c = 0.98$ is satisfied when As_4 tetrahedron is regular. Compared to Fig. 3 (a), magnitude of $\chi^c_{24,24}$ in Fig. 7 (a) is largely suppressed due to the reduction in the phonon-mediated interaction $g(0,\alpha)$ shown in Fig. 6 (b).

Figure 8 shows the α-dependence of λ_E for (a)$U = 0$ and $g(0) = 0.23$, and (b)$U = 1$ and $g(0) = 0.21$, respectively. In both cases, $\alpha_c = 0.98$ is satisfied when As_4 tetrahedron is regular. In case (a), the s_{++} state is always realized. In case (b), the s_{++} state is realized for $100° \leq \alpha \leq 120°$, whereas $s_\pm$ is realized for $\alpha \leq 95°$ or $125° \leq \alpha$, because the orbital fluctuations become inferior to spin fluctuations. In both (a) and (b), λ_E for s_{++} state rapidly decreases when bond angle α deviates from α_0. This result is consistent with the well-known experimental relationship between bond angle α and T_c [34, 45], and supports the realization of the orbital-fluctuation-mediated s_{++}-wave state in iron pnictides.

Finally, we note that the e-ph interaction due to As ion oscillation does not take the maximum value at $\alpha = \alpha_0$: For example, e-ph interaction by A_{1g}-mode, which is given by the change in the parameter b in Fig. 1 (a), will monotonically increase as α decreases. Therefore, the experimental relation between T_c and α strongly suggests that the iron pnictides are not conventional BCS superconductors due to charge fluctuations by A_{1g}-mode, but are the orbital-fluctuation-mediated superconductors due to Fe ion oscillations.

V. DISCUSSIONS

In previous sections, we have analyzed both s_{++}- and $s_{\pm}$-wave states based on the five-orbital HH model. Here, we discuss both states in more detail, by making comparison between theoretical results and experimental reports.

A. SC gap in the Z^2-orbital hole-pocket

Recently, bulk-sensitive ARPES measurements had been performed in (Ba,K)Fe_2As_2 and $BaFe_2(As,P)_2$ [36]. The observation have revealed the Z^2-orbital hole-pocket around $(0,0)$ at $k_z \sim \pi$ in the folded Brillouin zone ((π,π) in the unfolded Brillouin zone; see Fig. 4 (c)), which was predicted by the first principle LDA study around $k_z = \pi$ for larger bond angle α [46]. Moreover, it was found that the magnitude of the SC gap in the Z^2-orbital hole-pocket is as large as that in other hole-pockets composed of XZ/YZ- (and X^2-Y^2-) orbitals. However, the SC gap will strongly depend on the orbital nature of the FS parts in spin fluctuation mechanism, since the Z^2-orbital does not participate in the nesting [36].

Therefore, this "orbital-independent SC gap in (Ba,K)Fe_2As_2 and $BaFe_2(As,P)_2$" is a very crucial test for theories to understand the pairing mechanism. Here, we shift the Z^2-orbital level by +0.32eV in the present model to reproduce the Z^2-orbital hole-pocket at $k_z \sim \pi$ in the 3-dimensional model [46], and analyze the orbital dependence of the SC gap in detail.

Figure 9 (b) shows the $s_{\pm}$-wave SC gap functions obtained for $U = 1.0$ and $g(0) = 0$. The obtained parameter is $\lambda_E = 0.37$. (Note that λ_E for $s_{\pm}$-wave state decreases when Z^2-orbital hole pocket appears [2].) As we can see, spin-fluctuation scenario predicts very small SC gap on the Z^2-orbital FS, since the spin correlation between electrons in Z^2-orbital is very small: In iron pnictides, spin fluctuations due to the nesting are mainly induced by XZ/YZ-orbitals via intraorbital Coulomb interaction U between opposite spins. However, spin correlation between different orbitals is much weaker, since the Hund's coupling J is much smaller than U. For this reason, the SC gap in the Z^2-orbital hole-pocket is very small. Similar "orbital dependent SC gap" is considered to be realized in p-wave superconductor Sr_2RuO_4 [47].

On the other hand, strong orbital correlation exists for all d-orbitals in the present orbital-fluctuation scenario, since the e-ph interaction due to Fe-ion oscillation, Eq. (3), possesses many nonzero interorbital matrix elements. For this reason, the SC gap in the Z^2-orbital hole-pocket can be large. Figure 9 (c) shows the s_{++}-wave SC gap functions obtained for $U = 0$ and $g(0) = 0.20$ ($\alpha_c = 0.98$), induced by orbital fluctuations. The obtained parameters are $\lambda_E = 0.99$ and $\alpha_c = 0.98$. As expected, the SC gap on the Z^2-orbital FS becomes comparable with that on other FSs.

Therefore, the small orbital-dependence in the SC gap in (Ba,K)Fe_2As_2 and $BaFe_2(As,P)_2$ [36] supports the present orbital fluctuation scenario. For a quantitative study of this issue, large 3-dimensionality of the FSs in (Ba,K)Fe_2As_2 and $BaFe_2(As,P)_2$ may be important. This is an important issue for our future investigation.

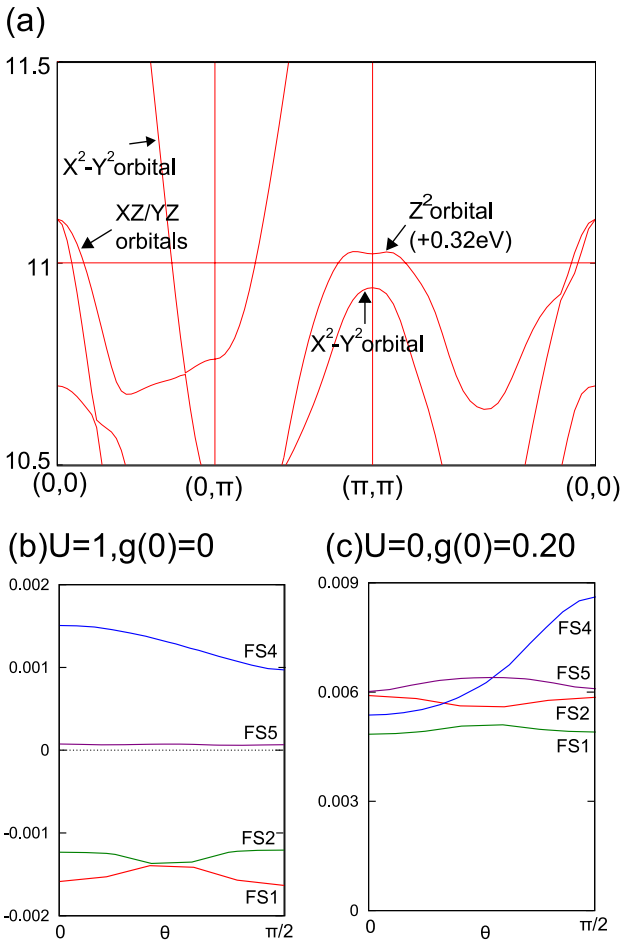

FIG. 9: (Color online) (a) Band structure (in the unfolded Brillouin zone) given by shifting the Z^2-orbital level by +0.32eV. The hole-pocket around (π,π), FS5 in Fig. 4(c), is composed of Z^2-orbital. (b) $s_{\pm}$-wave SC gap function for $U = 1.0$ and $g(0) = 0$. (c) s_{++}-wave SC gap function for $U = 0$ and $g(0) = 0.19$.

B. bond angle, pnictogen height

In Sec. IV, we have explained the experimental relation between the As-Fe-As bond angle α and λ_E in iron pnictides by assuming the s_{++}-wave SC state mediated by the orbital fluctuations. On the other hand, Kuroki *et al.* [46] had studied the same issue based on the spin fluctuation theory: In 1111 compounds, the Z^2-orbital hole pocket discussed in Sec. V A appears as the pnictogen hight $z = R_{\text{Fe-As}}\cos(\alpha/2)$ decreases. Then, λ_E for $s_{\pm}$-wave state quickly decreases, since Z^2-orbital does not contributes to the spin fluctuations. In this scenario, λ_E monotonically decreases as z does; The decrease in T_c

for $\alpha < \alpha_0$ cannot be explained without assuming the accidental balance between pnictogen height effect and another opposite effect.

In the present orbital fluctuation theory, $\lambda_{\rm E}$ for s_{++}-wave state is rather insensitive to the appearance of the Z^2-orbital hole-pocket since Z^2-orbital also contribute to the formation of the orbital fluctuations as discussed in Sec. V A. Therefore, $\lambda_{\rm E}$ or $T_{\rm c}$ will be mainly controlled by the bond angle α, which is consistent with the experimental report [34].

C. pressure effect on $T_{\rm c}$

We also discuss the pressure effect on $T_{\rm c}$ in iron pnictides. In $LaFeAsO_{1-y}F_x$, $T_{\rm c}$ increases from 26 K to 43 K in overdoped sample ($x = 0.14$) by applying $3 \sim 4$ GPa pressure [25]. In this case, both $1/T_1T$ and normal-state resistivity ρ around $T_{\rm c}$ are rather insensitive to the pressure [25, 48]. Similarly, $T_{\rm c}$ increases drastically in FeSe under pressure [45, 49]. On the other hand, $T_{\rm c}$ quickly decreases for $NdFeAsO_{1-y}$ and $TbFeAsO_{1-y}$ under pressure, accompanying the decrease in the temperature dependence of ρ (i.e, the inelastic scattering) [50].

To understand the pressure effect on $T_{\rm c}$, we would have to consider the change in the bandwidth $W_{\rm band}$, in addition to the bond angle α. In $NdFeAsO_{1-y}$ and $TbFeAsO_{1-y}$, the reduction in the inelastic scattering in ρ under pressure suggests the suppression of spin/orbital fluctuations. This change is expected to originate from the increase in $W_{\rm band}$, which drives the system toward weak-coupling regime. Then, reduction in spin/orbital fluctuations under pressure should make $T_{\rm c}$ lower.

Next, we discuss the possible origin of the enhancement in $T_{\rm c}$ under pressure. In FeSe, $T_{\rm c}$ increases under pressure $\sim$ 8GPa, whereas $\alpha_0 - \alpha (> 0)$ slightly increases. Here, we emphasize that the change in the Fe-As bond length $R_{\text{Fe-As}}$ would be the key parameter: Under pressure, the effective interaction due to e-ph coupling is given by $g(0) = (R^0_{\text{Fe-As}}/R_{\text{Fe-As}})^8 g^0(0)$, where the suffix 0 represents the quantity at ambient pressure. According to Ref. [49], $R^0_{\text{Fe-As}}/R_{\text{Fe-As}} = 2.38\mathring{\text{A}}/2.30\mathring{\text{A}}$ at 8GPa, and thus $g(0) \sim (4/3)g^0(0)$. This prominent enhancement in $g(0)$ under pressure might be the origin of strong increase of $T_{\rm c}$ in FeSe under pressure.

D. iron isotope effect

In Sec. III, we have discussed the iron isotope effect based on the orbital fluctuation scenario. Experimentally, Liu *et al.* reported that the iron isotope coefficient $\beta = -\partial \ln T_c / \partial \ln M$ is ~ 0.35 for $SmFeAsO_{0.85}F_{0.15}$ and $Ba_{0.6}K_{0.4}Fe_2As_2$ [51]. However, Shirage *et al.* had recently reported the negative (or zero) iron isotope effect for the same compounds; $\beta \sim -0.18$ for $(Ba,K)Fe_2As_2$ [35] and $\beta \sim -0.02$ for $SmFeAsO_y$ [52]. The reason for the discrepancy is yet unclear.

We have shown in Sec. III that the coefficient β changes from positive to negative as the Coulomb interaction increases. The first principle calculations had estimated that the ratio $U/W_{\rm band}$ for 122 compounds is larger than that for 1111 compounds [53]. Then, negative (zero) isotope effect reported for $(Ba,K)Fe_2As_2$ ($SmFeAsO_y$) does not contradict with the orbital fluctuation scenario.

In the spin fluctuation scenario, β becomes positive (negative) when the intra-pocket phonon-mediated attractive interaction $g(\mathbf{0}; \omega_l)$ is superior (inferior) to the inter-pocket one $g(\boldsymbol{Q}; \omega_l)$ [54, 55]. Therefore, sign change in β can be explained if the nature of e-ph interaction largely depends on the compounds.

VI. SUMMARY

In the present paper, we studied the five-orbital HH model for iron pnictides, and found that s_{++}-wave SC state is induced by orbital fluctuations in the presence of small e-ph interaction ($\lambda \lesssim 0.15$). Strong orbital fluctuations are induced by multiple scattering processes due to the e-ph interaction, involving all five d-orbitals on the FSs. We stress that the second-order process alone, which is usually studied in conventional BCS analysis [28], can neither induce large orbital fluctuations nor high-$T_{\rm c}$ s_{++}-wave SC state. Roughly speaking, $T_{\rm c}$ in the orbital fluctuation theory would be given as $T_{\rm c} \sim \omega_{\rm D} \exp(-1/\lambda^*)$, where $\lambda^* \sim \lambda(1 - \alpha_{\rm c})^{-1}$ is the enhanced coupling constant, and thus it is much larger than $T_{\rm c}^{\rm BCS} \sim \omega_{\rm D} \exp(-1/\lambda)$.

The virtue of this theory is that we can also explain the following issues which remain unresolved within the spin fluctuation theory: (i) empirical relationship between $T_{\rm c}$ and the As-Fe-As bond angle (Lee plot), (ii) negative iron isotope effect in (Ba,K)Fe2As2, and (iii) orbital-independent SC gap in $(Ba,K)Fe_2As_2$ and $BaFe_2(As,P)_2$ observed by bulk-sensitive ARPES measurement [36]. Recently, theoretically predicted orbital fluctuations in Figs. 3 (a) and (b) had been confirmed by the softening of the elastic constants C_{44} and $C_{\rm E}$ [30]. These obtained results support the idea of the s_{++}-wave state mediated by orbital fluctuations in iron pnictides, next to the orbital-ordered state in mother compounds.

Finally, we list several significant future issues. The e-ph interaction due to corrective oscillations (e.g., half-breathing mode) might be important to increase the s_{++}-wave $T_{\rm c}$. To make quantitative comparison between s_{++}-wave and $s_{\pm}$-wave states, study of the self-energy and vertex corrections for $\chi^{c(s)}$ and the Eliashberg gap equation is highly desired. The FLEX approximation would be useful for this purpose [40].

Acknowledgments

We are grateful to D.S. Hirashima, M. Sato, Y. Kobayashi, Y. Matsuda, T. Shibauchi, M. Takigawa, S. Shin, T. Shimojima, Y. Ōno, F.C. Zhang, and M. Yoshizawa for useful comments and discussions. This study has been supported by Grants-in-Aid for Scientific Research from MEXT of Japan, and by JST, TRIP. Numerical calculations were performed using the facilities of the supercomputer center, Institute for Molecular Science.

Appendix A: Phase Diagram and Orbital Fluctuations for $J/U > 1/6$

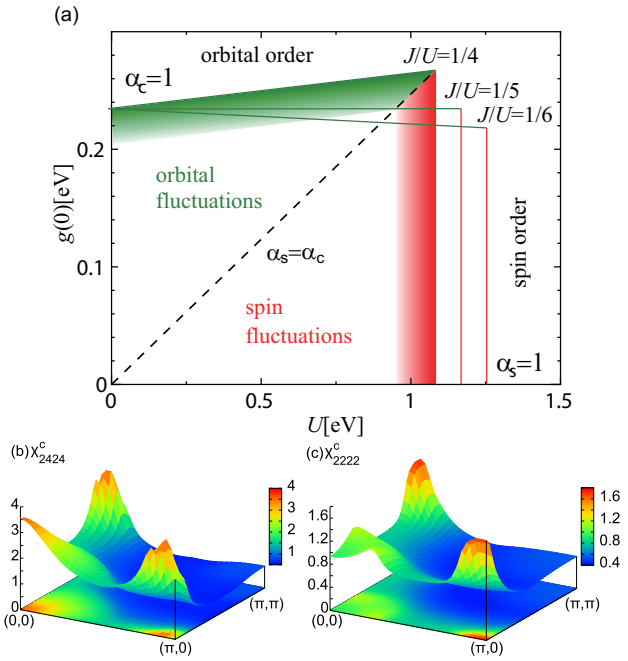

FIG. 10: (Color online) (a) Obtained U-$g(0)$ phase diagram for $J/U = 1/4$, 1/5 and 1/6. (b) Obtained $\chi^{c}_{24,24}(\boldsymbol{q}, 0)$ for $J/U = 1/6$ and $n = 6.1$. (c) Obtained $\chi^{c}_{22,22}(\boldsymbol{q}, 0)$ for $J/U = 1/6$ and $n = 6.1$.

In the present paper, we studied the multiorbital HH model for general parameters under the constraint $J/U = 1/6$. In fact, based on the first-principle calculation, Miyake *et al.* had derived the averaged J/U as 0.4eV/2.5eV=1/6.3 for LaFeAsO and 0.45eV/3eV=1/6.7 for $BaFe_2As_2$, respectively [53]. Moreover, very small value of $J/U < 0.1$ is required to reproduce the small magnetic moment in the SDW state within the mean-field approximation [56]. However, J/U is expected to be larger for usual iron-compounds, and there is no consensus on the value of J/U in iron pnictides up to now. In case of $J/U = 1/6$, Coulomb interaction enhances the orbital fluctuations when $g(0)$ is fixed, as shown in Fig. 2. However, it is highly desired to study the orbital fluctuation for general value of J/U. In this appendix, we discuss this issue using the RPA, and show that characteristic nature of orbital fluctuations does not influenced by J/U.

Figure 10 (a) represents the U-$g(0)$ phase diagram given by the mean-field approximation for $J/U = 1/4$, 1/5 and 1/6. For $J/U = 1/4$, the Coulomb interaction reduces the charge Stoner factor α_c when $g(0)$ is fixed, indicating the suppression of orbital fluctuations. The value of $g_{\rm cr}(0)$ for $\alpha_c = 1$ is 0.26 when $U = 1.0$; the corresponding dimensionless coupling $\lambda \equiv gN(0)$ is only 0.18. For $J/U = 1/5$, α_c is almost independent of U. Therefore, the value of $g_{\rm cr}(0)$ increases with J/U: The reason is that U ($U' = U - 2J$) reduces (enhances) orbital fluctuations. As for the spin correlation, the value of $U_{\rm cr}$ for $\alpha_s = 1$ decreases with J/U, indicating the enhancement of spin fluctuations.

Figure 10 (b) and (c) show the obtained $\chi^{c}_{24,24}(\boldsymbol{q}, 0)$ and $\chi^{c}_{22,22}(\boldsymbol{q}, 0)$ for $J/U = 1/4$, $U = 1$, and $a_c = 0.98$ ($g(0) \approx 0.26$) at $T = 0.02$. Comparing with Figs. 3 (a) and (b), it is found that the orbital susceptibilities are almost independent of $J/U \leq 1/4$ for a fixed α_c. Thus, the present orbital fluctuation scenario for iron pnictides would be plausible for $J/U \leq 1/4$.

[1] Y. Kamihara, T. Watanabe, M. Hirano, and H. Hosono, J. Am. Chem. Soc. **130**, 3296 (2008).
[2] K. Kuroki, S. Onari, R. Arita, H. Usui, Y. Tanaka, H. Kontani and H. Aoki, Phys. Rev. Lett. **101**, 087004 (2008).
[3] I. I. Mazin, D. J. Singh, M. D. Johannes, and M. H. Du, Phys. Rev. Lett. **101**, 057003 (2008).
[4] T. Moriya, Y. Takahashi, and K. Ueda, J. Phys. Soc. Jpn. **59**, 2905 (1990). K. Ueda, T. Moriya and Y. Takahashi, J. Phys. Chem. Solids. **53**, 1515 (1992).
[5] P. Monthoux and D. Pines, Phys. Rev. B **47**, 6069 (1993).
[6] N. E. Bickers and S. R. White, Phys. Rev. B **43**, 8044 (1991).
[7] J. Schmalian, Phys. Rev. Lett. **81**, 4232 (1998).
[8] H. Kino and H. Kontani, J. Phys. Soc. Jpn. **67**, 3691 (1998).
[9] H. Kondo and T. Moriya, J. Phys. Soc. Jpn. **67**, 3695 (1998).
[10] T. Takimoto, T. Hotta, and K. Ueda, Phys. Rev. B **69**, 104504 (2004).
[11] S. Onari, and H. Kontani, Phys. Rev. Lett. **103**, (2009) 177001.
[12] A. Kawabata, S. C. Lee, T. Moyoshi, Y. Kobayashi and M. Sato, J. Phys. Soc. Jpn. **77**, 103704 (2008); M. Sato,

Y. Kobayashi, S. C. Lee, H. Takahashi, E. Satomi and Y. Miura, J. Phys. Soc. Jpn. **79**, 014710 (2009); S.C. Lee, E. Satomi, Y. Kobayashi, and M. Sato, J. Phys. Soc. Jpn. **79**, 023702 (2010).

[13] C. Tarantini, M. Putti, A. Gurevich, Y. Shen, R. K. Singh, J. M. Rowell, N. Newman, D. C. Larbalestier, P. Cheng, Y. Jia, and H.-H. Wen, Phys. Rev. Lett. **104**, 087002 (2010).

[14] Y. Nakajima, T. Taen, Y. Tsuchiya, T. Tamegai, H. Kitamura, and T. Murakami, arXiv:1009.2848.

[15] Y. Li, J. Tong, Q. Tao, C. Feng, G. Cao, W. Chen, F.C. Zhang, and Z.A. Xu, New J. Phys. **12** (2010) 083008.

[16] S. Iikubo, M. Ito, A. Kobayashi, M. Sato and K. Kakurai, J. Phys. Soc. Jpn. **74**, 275 (2005).

[17] M. Ito, H. Harashina, Y. Yasui, M. Kanada, S. Iikubo, M. Sato, A. Kobayashi and K. Kakurai, J. Phys. Soc. Jpn. **71**, 265 (2002).

[18] H. F. Fong, P. Bourges, Y. Sidis, L. P. Regnault, A. Ivanov, G. D. Gu, N. Koshizuka and B. Keimer, Nature **398**, 588 (1999).

[19] C. Stock, C. Broholm, J. Hudis, H. J. Kang, and C. Petrovic, Phys. Rev. Lett. **100**, 087001 (2008).

[20] A. D. Christianson, E. A. Goremychkin, R. Osborn, S. Rosenkranz, M. D. Lumsden, C. D. Malliakas, I. S. Todorov, H. Claus, D. Y. Chung, M. G. Kanatzidis, R. I. Bewley and T. Guidi, Nature **456**, 930 (2008).

[21] Y. Qiu, W. Bao, Y. Zhao, C. Broholm, V. Stanev, Z. Tesanovic, Y. C. Gasparovic, S. Chang, J. Hu, B. Qian, M. Fang and Z. Mao, Phys. Rev. Lett. **103**, 067008 (2009).

[22] D. S. Inosov, J. T. Park, P. Bourges, D. L. Sun, Y. Sidis, A. Schneidewind, K. Hradil, D. Haug, C. T. Lin, B. Keimer and V. Hinkov, Nature Physics **6** 178 (2010).

[23] S. Onari, H. Kontani and M. Sato, Phys. Rev. B 81, 060504(R), (2010).

[24] Y. Nakai, T. Iye, S. Kitagawa, K. Ishida, H. Ikeda, S. Kasahara, H. Shishido, T. Shibauchi, Y. Matsuda, and T. Terashima, Phys. Rev. Lett. **105**, 107003 (2010).

[25] T. Nakano, N. Fujiwara, K. Tatsumi, H. Okada, H. Takahashi, Y. Kamihara, M. Hirano, and H. Hosono, Phys. Rev. B **81**, 100510(R) (2010).

[26] H. Kontani and S. Onari, Phys. Rev. Lett. **104**, 157001 (2010).

[27] Y. Yanagi and Y. Yamakawa, and Y. Ōno, Phys. Rev. B **81**, 054518 (2010).

[28] L. Boeri, O. V. Dolgov, A. A. Golubov, Phys. Rev. Lett. **101**, 026403 (2008).

[29] R. M. Fernandes, L. H. VanBebber, S. Bhattacharya, P. Chandra, V. Keppens, D. Mandrus, M. A. McGuire, B. C. Sales, A. S. Sefat, J. Schmalian, arXiv:0911.3084.

[30] M. Yoshizawa, R. Kamiya, R. Onodera, Y. Nakanishi, K. Kihou, H. Eisaki, and C. H. Lee, arXiv:1008.1479.

[31] M. Rahlenbeck, G. L. Sun, D. L. Sun, C. T. Lin, B. Keimer, C. Ulrich, Phys. Rev. B **80**, 064509 (2009).

[32] A. A. Kordyuk, V. B. Zabolotnyy, D. V. Evtushinsky, T. K. Kim, I. V. Morozov, M. L. Kulic, R. Follath, G. Behr, B. Buechner, and S. V. Borisenko, arXiv:1002.3149.

[33] T. Dong, Z. G. Chen, R. H. Yuan, B. F. Hu, B. Cheng, and N. L. Wang, arXiv:1005.0780.

[34] C.-H. Lee, A. Iyo, H. Eisaki, H. Kito, M. T. Fernandez-Diaz, T. Ito, K. Kihou, H. Matsuhata, M. Braden, and K. Yamada, J. Phys. Soc. Jpn. **77**, 083704 (2008).

[35] P. M. Shirage, K. Kihou, K. Miyazawa, C.-H. Lee, H. Kito, H. Eisaki, T. Yanagisawa, Y. Tanaka and A. Iyo, Phys. Rev. Lett. **103**, 257003 (2009).

[36] T. Shimojima, private communication.

[37] T. Shimojima, K. Ishizaka, Y. Ishida, N. Katayama, K. Ohgushi, T. Kiss, M. Okawa, T. Togashi, X.-Y. Wang, C.-T. Chen, S. Watanabe, R. Kadota, T. Oguchi, A. Chainani, and S. Shin, Phys. Rev. Lett. **104**, 057002 (2010).

[38] J.-H. Chu, J. G. Analytis, K. D. Greve, P. L. McMahon, Z. Islam, Y. Yamamoto, I. R. Fisher, arXiv:1002.3364; A. Dusza, A. Lucarelli, F. Pfuner, J.-H. Chu, I. R. Fisher, and L. Degiorgi, arXiv:1007.2543.

[39] T. Takimoto, T. Hotta, T. Maehira and K. Ueda, J. Phys. Condens. Matter **14**, L369 (2002).

[40] S. Onari and H. Kontani, arXiv:1009.3882.

[41] K. Hashimoto, M. Yamashita, S. Kasahara, Y. Senshu, N. Nakata, S. Tonegawa, K. Ikada, A. Serafin, A. Carrington, T. Terashima, H. Ikeda, T. Shibauchi and Y. Matsuda, Phys. Rev. B **81**, 220501(R) (2010).

[42] P. Morel and P. W. Anderson, Phys. Rev. **125**, 1263 (1962).

[43] P. B. Allen and B. Mitrović, Solid State Physics **37**, 1 (1982).

[44] H. Kontani and M. Ohno, Phys. Rev. B **74**, 014406 (2006).

[45] Y. Mizuguchi, Y. Hara, K. Deguchi, S. Tsuda, T. Yamaguchi, K. Takeda, H. Kotegawa, H. Tou and Y. Takano, Supercond. Sci. Technol. **23**, 054013 (2010).

[46] K. Kuroki, H. Usui, S. Onari, R. Arita, H. Aoki, Phys. Rev. B **79**, 224511 (2009).

[47] D.F. Agterberg, T.M. Rice, and M. Sigrist, Phys. Rev. Lett. **78**, 3374 (1997).

[48] T. Takahashi, K. Igawa, K. Arii, Y. Kamihara, M. Hirano and H. Hosono, Nature **453**, 376 (2008).

[49] S. Margadonna, Y. Takabayashi, Y. Ohishi, Y. Mizuguchi, Y. Takano, T. Kagayama, T. Nakagawa, M. Takata and K. Prassides, Phys. Rev. B **80**, 064506 (2009).

[50] N. Takeshita, A. Iyo, H. Eisaki, H. Kito, and T. Ito, J. Phys. Soc. Jpn. **77** 075003 (2008).

[51] R. H. Liu, T. Wu, G. Wu, H. Chen, X. F. Wang, Y. L. Xie, J. J. Ying, Y. J. Yan, Q. J. Li, B. C. Shi, W. S. Chu, Z. Y. Wu and X. H. Chen, Nature **459**, 64 (2009).

[52] P. M. Shirage, K. Miyazawa, K. Kihou, H. Kito, Y. Yoshida, Y. Tanaka, H. Eisaki and A. Iyo, Phys. Rev. Lett. **105**, 037004 (2010).

[53] T. Miyake, K. Nakamura, R. Arita and M. Imada, J. Phys. Soc. Jpn. **79** 044705 (2010).

[54] T. Yanagisawa, K. Odagiri, I. Hase, K. Yamaji, P. M. Shirage, Y. Tanaka, A. Iyo and H. Eisaki, J. Phys. Soc. Jpn. **78**, 094718 (2009).

[55] Y. Bang, Phys. Rev. B **79**, 092503 (2009).

[56] E. Bascones, M.J. Calderon, and B. Valenzuela, Phys. Rev. Lett. **104**, 227201 (2010).